Iranian Journal of Astronomy and Astrophysics
Vol. 12, No. 4, Autumn 2025, 335–346
©Available online at http://ijaa.du.ac.ir
DOI: 10.22128/ijaa.2026.3311.1247
Online ISSN: 2383–403X

Iranian Journal of Astronomy and Astrophysics

Research Paper

The Effect of Temperature Anisotropy on Ignition Conditions of Advanced Fuel Degenerate Plasma in the Presence of a Magnetic Field in Nuclear Fusion Configurations

Majid Bakhtiyari[1] · Mohammad Mahdavi*[2] · Fatemeh Khodadadi Azadboni[3]

[1] Department of Physics, Faculty of Basic Sciences, University of Mazandaran, P.O. Box 47415-416, Babolsar, Iran;
E-mail: m.bakhtiyari01@umail.umz.ac.ir

[2] Department of Physics, Faculty of Basic Sciences, University of Mazandaran, P.O. Box 47415-416, Babolsar, Iran;
*E-mail: m.mahdavi@umz.ac.ir

[3] Department of Physics Education, Farhangian University, P.O. Box 14665-889, Tehran, Iran;
E-mail: fatemehnejadtaghi98@gmail.com

Received: 4 May 2026; **Accepted:** 14 July 2026; **Published:** 15 July 2026

Abstract. The investigation of the impact of effective parameters on optimizing fuel pellet ignition conditions in nuclear fusion is one of the important topics in nuclear power generation cycles. ICF and MIF are two advanced methods for nuclear power generation. This paper investigates the influence of temperature anisotropy and external magnetic fields on the ignition conditions of advanced Deuterium-Helium-3 $(D -^3 He)$ fuel pellets within degenerate plasma, specifically under Inertial Confinement Fusion (ICF) and Magneto-Inertial Fusion (MIF) regimes. Since the degeneration condition is fulfilled at low temperatures and high densities, it is expected that better ignition will be achieved by reducing the electron temperature. Calculations show that applying an external magnetic field to the $(D -^3 He)$ fuel pellet plasma increases the surface density by a factor of five in the magnetized inertial fusion (MIF) state compared to the inertial confinement fusion (ICF) state, while maintaining the stability of the plasma degenerate conditions. This increase in the surface density of the fuel leads to an increase in the energy deposition of alpha particles into the plasma environment of the fuel pellet. In addition, it has been shown that by applying temperature anisotropy to the fuel pellet, the plasma electron temperature in the MIF mode is reduced by 70%, surpassing the reduction observed in ICF mode. The reduction in the electron temperature of the plasma environment, decreases the dissipated bremsstrahlung power, while simultaneously increasing the plasma temperature of the fuel pellet thereby facilitating more effective ignition of the $(D -^3 He)$ fuel pellet.

Keywords: Nuclear Fusion Configurations, Degenerate Fuel, Temperature Anisotropy, Advance Fuel, Surface Density Fuel.

1 Introduction

The deuterium-tritium (D-T) fuel cycle presents unique challenges in the design of fusion reactors. The 14MeV neutrons produced in the D-T reaction and the presence of tritium in

---

* *Corresponding author*

the fuel cycle are two important issues. 14MeV neutrons damage reactor wall components, reduce their useful life, activate reactor wall materials, and lead to large accumulations of radioactive waste. Tritium does not occur in nature, but can be produced by the reaction $n +^6$ Li $\rightarrow$ T + α. The production of tritium and the large accumulation of tritium raise safety concerns [1]. Advanced alternative fuel cycles have been under investigation for many years. Two major motivations for researchers to replace D-T fuel with advanced fuel are: first, to eliminate tritium from the fuel cycle in order to simplify the fuel cycle; and second, to mitigate or substantially reduce neutron production in the fusion reactors thereby minimizing radiation-induced structural damage and component activation within fusion reactors [2]. Of all the advanced fuels available, deuterium-helium-3 (D-^{3}He) is the most notable. While no neutrons are produced in this fuel reaction, neutron production is unavoidable through the deuterium-deuterium (D-D) side reaction and the secondary D-T reaction. The neutrons produced are mostly of lower energy, with the 2.45 MeV neutrons from D-D reactions being less destructive than the 14 MeV neutrons from D-T reactions. Studies have shown that the D-^{3}He fuel cycle largely solves the problems of reduced reactor component lifetimes associated with neutron damage, while neutron activation and the associated radioactive waste generation remain a concern. The D-^{3}He fuel cycle avoids the need for tritium. ^{3}He is not abundant on Earth in sufficient quantities to support the fusion energy industry. However, ^{3}He can be found on the lunar surface, and proponents of the D-^{3}He fuel cycle suggested that extracting ^{3}He from the lunar surface and transporting it to Earth to fuel a fusion energy industry may be economical [3].

Currently, studies in the field of inertial confinement fusion (ICF) are being developed within the framework of two concepts of volumetric ignition and fast ignition, namely, hydrodynamic spark ignition, including ignition by a focused shock wave. These concepts are based on different methods for coordinating the processes of plasma compression and heating and different methods for the formation of the igniter [4]. ICF targets are compressed using short-wavelength laser radiation with wavelengths $\lambda \leq 1$ μm, and a decrease in the wavelength increases the efficiency of the laser-target interaction. A decrease in the radiation wavelength leads to an increase in the critical plasma density, at which the frequency of the laser radiation is equal to the plasma frequency. Therefore, the density of the plasma region in which the laser radiation is absorbed increases. This leads to an increase in the inverse absorption coefficient of bremsstrahlung and the erosion pressure.

The concept of fast ignition was first proposed in 1994 by Tabak, Morrow and Lindell. They proposed that ignition of the compressed fuel in the central region is achieved by a short, high-intensity laser pulse [5]. In this concept, it was proposed to fundamentally separate the compression and laser heating processes in time due to the simultaneous action of pulses from two drivers with different intensities on the target. The first driver, a broad nanosecond laser pulse with slow precompression provides the entire thermonuclear fuel along a "cold adiabatic curve" to a density of several hundred grams per cubic centimeter. The second driver, a short pulse with a duration of several tens of picoseconds, acts on the target at the moment of maximum compression and, during the inertial confinement time, heats a small area of the compressed plasma to thermonuclear temperatures, thereby providing the formation of an igniter and subsequent ignition of the target [6]. Another important advantage of fast ignition which can be decisive in solving the ICF problem, is that when the ignition zone is formed only due to hydrodynamic accumulation after compression of a spherical target, the hydrodynamic Rayleigh-Taylor instability can exert a serious negative effect since the peripheral zone of the dense thermonuclear fuel is slowed down by the low-density material of the central part of the target [7]. The onset of this instability can lead to mixing of different regions of the target (including the central and peripheral fuel regions) during compression. As a result, the central fuel region may not heat up to the thermonuclear temperature. Experience gained in ICF studies shows that hydrodynamic instability is a serious problem that can be solved only if strict requirements for the quality of target construction and the homogeneity of its irradiation by the launch beams are met [8]. At present, the stability of the target compression is, in general, the only problem of ICF that has not yet been fully solved. As will be discussed below, even if the homogeneity of the target radiation provided in the indirect compression flow is very high, the violation of the compression stability prevents the experimental demonstration of spark ignition. In the fast ignition scheme, the formation of the igniter is not related to the compression of the target. Moreover, mixing the central and peripheral regions of the fuel in the pre-compression flow of the target can even be beneficial, as it can lead to a higher degree of fuel homogeneity, so that, despite the need to use an additional ignition initiator, fast ignition can be the only possible method for efficient spark ignition formation. Fast ignition occupies a central place in laser-driven ICF projects in the world's largest laboratories. It is well known that the laser energy currently achieved in ICF studies reaches several megajoules, which allows the ignition of a fusion target [9,10]. In the mid-2000s, two projects focusing on laser energy were proposed. Their goal was not only to demonstrate ignition, but also to achieve high achievements in fast ignition of direct compression targets. Two examples of experimental projects realizing fast ignition are given in references [11,12]. The idea of using a magnetic field to control thermal conductivity was first proposed by Landshoff at Los Alamos National Laboratory (LANL) around 1945 [13]. Furthermore, experimental progress over the past three decades has been such that some who are sufficiently familiar with magnetic target fusion (MTF) or magnetic inertial fusion (MIF) believe that an incontrovertible proof-of-principle test is now possible. MIF involves the hydrodynamic compression of a hot, confined magnetic target plasma to ignition conditions. MIF also takes advantage of two advantages of a magnetic field in a plasma: first, it reduces thermal conductivity; and second, it effectively increases the energy deposition of the charged particle reaction product in the plasma. To ensure that thermal conduction remains the primary energy loss mechanism, we have modeled the initial fuel density at levels significantly lower than those typically employed in inertial confinement fusion (ICF), thereby minimizing radiant energy losses from the plasma. This allows the targets to be larger, and the reduced losses provide a lower compression rate, so that the internal detonation time can be long and the required power and intensity on the target can be very low. The parameter space for MIF lies between ICF and magnetic confinement for fusion energy (MFE) in terms of density and time scale. While the energy requirements for igniting a magnetized target are comparable to those of an inertial confinement fusion (ICF) target of equivalent fuel mass, the demands for power and power density are significantly reduced. Consequently, existing pulsed-power facilities may possess the capability to achieve ignition in magnetized inertial fusion (MIF) targets. Ignition of a cold fuel layer by a burning central magnetic fuel should significantly increase the yield of a magnetic fuel target [14].

In this study, first in Section 2, the parameters of thermal anisotropy and degradation are introduced in the plasma of the $(D-^3He)$ fuel pellet; then in Section 3, using the heating and cooling power density relations, the ignition condition and surface density are presented in accordance with the physical conditions of the fuel in the ICF and MIF processes. Analysis of results is presented in Section 4. Finally, in Section 5, conclusions are presented.

2 Degenerate conditions and temperature anisotropy in fuel pellet plasma

Compared to inertial fusion, the presence of external magnetic fields in inertial-magnetic fusion reduces plasma medium density and particle thermal transport, which results in increased alpha particle energy deposition into the plasma. Ultimately, this reduces the surface density and increases the hydrodynamic instabilities of the plasma medium. In the MIF, since the fuel compression and ignition processes are carried out in separate stages, it is possible to achieve low-temperature, high-density plasma during compression [15].

2.1 Degenerate conditions in plasma

In dense and low-temperature plasmas, due to the small distance between electrons and the weak interaction between them, the quantum mechanical effects dominate the behavior of the electron gas, and the electrons will behave very much like a degenerate electron gas [16]. The equations that predict the behavior of these plasmas differ from the classical plasma equations. For example, due to the Pauli exclusion principle, the bremsstrahlung emission in degenerate plasmas is greatly reduced compared to classical plasmas; this reduction occurs as the plasma ignition temperature decreases [17]. The Fermi energy, ε_f, as the maximum energy of a filled level, is given by [18]

$$\varepsilon_f = \frac{1}{8}\frac{h^2}{m_e}(\frac{3n_e}{\pi})^{2/3} = 2.19 \times 10^{-15} n_e^{2/3} \text{ [eV]}, \tag{1}$$

where n_e and m_e represent the electron number density and electron mass respectively. The degeneracy parameter (η) can be defined as the necessary condition for creating a degeneracy state in the fuel plasma based on the ratio between the Fermi energy and the thermal energy

$$\eta = \frac{\varepsilon_f}{T_e}. \tag{2}$$

If $\eta > 1$, the electrons are in a degenerate state. Therefore, the most important condition for degenerate conditions during the burning process is that the electron temperature should be lower than the Fermi temperature [18].

2.2 Temperature anisotropy conditions in plasmas

Fast ignition is known as a highly efficient method for the progression of ICF concepts. In the fast ignition method, hot electrons generated by the laser-plasma interaction provide the power density required to ignite the fuel pellet. The electron beams generated at the critical density level generate a shock wave as an ignitor for the condensed fuel. The intense shock wave exerts high pressure on the fuel plasma and leads to temperature anisotropy. The presence of temperature anisotropy may lead to the formation of electromagnetic instabilities, including Weibel instability, in the plasma medium of the fuel pellet [19,20]. For the asymmetric temperature distribution function ($T_{e\perp} \neq T_{e\parallel}$) (where the parallel temperature axis of electrons is considered as; $T_{e\parallel} = T_{ez}$, and the vertical temperature component of electrons is also chosen proportional to the x-y plane), if the vertical temperature component of electrons is greater than the parallel temperature component of electrons ($T_{e\perp} > T_{e\parallel}$ or $T_\perp > T_\parallel$), it causes electromagnetic instability. These instabilities propagate electromagnetic waves along the magnetic field. In the condition ($T_\parallel > T_\perp$), it produces waves along the parallel temperature component of electrons, causing temperature anisotropy in the distribution function [20]. The ignition conditions of the fuel plasma and the deposition of radiation energy in the fuel plasma can be affected by these instabilities and temperature anisotropies. This study investigates the ignition conditions for D-^{3}He fuel in ICF and MIF processes, taking into account the temperature anisotropy of electrons under conditions where the electron and ion temperatures are not equal. The interaction of the laser pulse with the fuel pellet plasma heats the fuel plasma in the velocity dimension along the direction of wave propagation, which leads to temperature anisotropy in the electron temperature distribution. The laser beam generates a shock wave in the fuel, where the ion and electron temperatures differ. The electron's temperature anisotropy parameter is represented by $\beta = T_\perp/T_\parallel$, in which case, $T_e = T_\perp^{2/3} T_\parallel^{1/3}$ can be expressed as $T_e = \beta^{2/3} T_\parallel$; hence this relation will be used for the electron temperature in all calculations.

3 Hot spot ignition conditions of the D-^{3}He fuel pellet

The reaction of D-^{3}He fuel pellet , which results in the production of an alpha particle along with a proton, is as follows

$$\mathrm{D} +^3 \mathrm{He} \rightarrow \alpha(3.6\mathrm{MeV}) + \mathrm{P}(14.7\mathrm{MeV}).$$

The following three reactions are also considered side reactions because they have fusion cross sections that are proportional to the D-^{3}He fuel

$$\begin{aligned} &\mathrm{D} + \mathrm{T} \rightarrow \alpha(3.5\mathrm{MeV}) + \mathrm{n}(14.1\mathrm{MeV}),\\ &\mathrm{D} + \mathrm{D} \rightarrow \mathrm{T}(1.01\mathrm{MeV}) + \mathrm{P}(3.02\mathrm{MeV}),\\ &\mathrm{D} + \mathrm{D} \rightarrow \mathrm{n}(2.45\mathrm{MeV}) +^3 \mathrm{He}(0.82\mathrm{MeV}). \end{aligned}$$

The other reactions possible are neglected because they have very small fusion cross sections compared to the D-^{3}He reaction. The difference between the ICF and MIF processes is the presence of cyclotron radiation power density in the MIF process, which is included in the MIF dynamic state equations. The ignition condition for the $(D-^3He)$ fuel pellet is obtained by introducing the generated and loss power densities, which can be calculated as follows [21]

$$W_f - W_{loss} \geq 0, \tag{3}$$

where W_f represents the fusion power density and W_{loss} represents the loss power density (loss powers density consisting of Bremsstrahlung power density, W_B, Mechanical work, W_{me}, thermal conduction of electrons, W_{he} , and Cyclotron radiation, W_{cy}). These are discussed below.

The fusion power density for a D-^{3}He fuel pellet is given by [21]

$$W_f \left[\frac{\mathrm{erg}}{\mathrm{cm^3 s}}\right] = n_D n_{^3\mathrm{He}} < \sigma v >_{\mathrm{D^3He}} E, \tag{4}$$

where n_D and $n_{^3\mathrm{He}}$ are the number densities of Deuterium and Helium-3, respectively, and E is the fusion energy. $< \sigma v >_{\mathrm{D^3He}}$ is the reactivity of the D-^{3}He reaction [22]. Bremsstrahlung is one of the most important energy loss mechanisms in achieving ignition and can be introduced as follows [17]

$$W_B \left[\frac{\mathrm{erg}}{\mathrm{cm^3 s}}\right] = \frac{K(T_e)^2}{h} \left[F_1(\eta) - \frac{1}{2}\ln^2(e^\eta + 1)\right], \tag{5}$$

and

$$K = \left(\frac{256\pi^3}{3\sqrt{3}}\right)\left(\frac{1}{4\pi\varepsilon_0}\right)^3 \frac{Z^2 e^6 n_i}{h^3 c^3}. \tag{6}$$

In equation (6), n_i and e represent the ionic number density and electron charge respectively. When the driver beam hits the hot spot, the temperature of the fuel plasma increases. On the other hand, the density of the hot spot is equal to the density of the surrounding cold fuel, so a pressure difference is created between the hot spot and the main fuel causing the hot spot to do mechanical work on its surroundings and lose some of its energy this way. The ultimate pressure is introduced as follows [23]

$$P = \frac{n_e k_B T_e + \sum_i n_i k_B T_i}{V}, \tag{7}$$

k_B represents Boltzmann's constant. The mechanical work power density of electrons and ions in the degenerate state is as follows [24]

$$W_{me}\left(\frac{\text{erg}}{\text{cm}^3\ \text{s}}\right) = \frac{4\pi C_s R^2 n_e k_B T_e}{V} \tag{8}$$

$$W_{mi}\left(\frac{\text{erg}}{\text{cm}^3\ \text{s}}\right) = \frac{4\pi C_s R^2 n_i k_B T_i}{V} \tag{9}$$

where V and R are the volume and radius of the hot spot. In terms of mechanical power density, the speed of sound is $C_s = \sqrt{\gamma P/\rho}$, where $\gamma = 3/5$.

The electron thermal conductivity in a degenerate plasma is written as follows [18]

$$W_{he}\left(\frac{\text{erg}}{\text{cm}^3\ \text{s}}\right) = 3A_e \frac{(T_e)^{7/2}}{R^2 \log\Lambda Z_i(1+3.3Z_i)}, \tag{10}$$

where $A_e = 5.529 \times 10^{28}(\text{keV}^{-5/2}\text{cm}^{-1}\text{s}^{-1})$ and $\log\Lambda$ represents the Coulomb logarithm in the decay plasma

$$\log\Lambda = \text{Log}\left[0.1718 n_e^{-1/3}\rho_c\right], \qquad \rho_c = \frac{z_i z_j e^2}{2E_\alpha}.$$

The indices i and j indicate the types of ions. To obtain the ignition condition of the MIF process, the cyclotron power density must also be included in the calculations, which is represented by the following equation [23]

$$W_{cy}\left(\frac{\text{erg}}{\text{cm}^3\ s}\right) = \frac{4e^4 k_B}{3m_e^3 c^5} B^2 n_e T_e, \tag{11}$$

where B represents the intensity of the magnetic field in which the electrons are spinning.

4 Analysis of results

The ignition condition and allowable surface density regions of D-^{3}He fuel in the ICF mode can be calculated by substituting the generated and loss power densities (equations (4)-(9)) into equation (3). By estimating the Fermi energy of the plasma media of the D-^{3}He fuel pellet to be 3.9 keV, the degenerate condition requires that the electron temperature of the environment be less than 3.9 keV. In Figure (1) it can be seen that in the case of a partially degenerate plasma ($\eta \approx 2$), in the ICF state, the electron temperature of the fuel pellet is smaller than the Fermi temperature of the plasma when the surface density increases from

ρR $= 10$g$/cm^2$ to ρR $= 100$g$/cm^2$, for an ion temperature range of 100 keV. In other words, in the ion temperature range of 100 keV, the electron temperature will not change much, and the fuel pellet plasma will remain in a degenerate state. Therefore, the surface density ρR $= 100$g$/cm^2$ can be considered as the optimal surface density in the ICF mode. So, the optimal value of the magnetic field intensity in the MIF mode for the partial degenerate plasma ($\eta \approx 2$) can be calculated by adding the cyclotron loss power (equation (10)) to the ignition condition equation (equation (3)) for the surface density ρR $= 100$g$/cm^2$ applying the magnetic field intensity to the conditions governing the D-^{3}He fuel pellet.

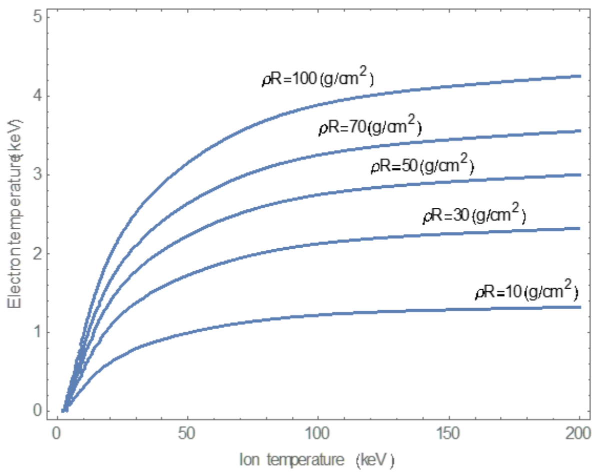

Figure 1: Variation of electron temperature with respect to ion temperature in D-^{3}He fuel under ICF mode for a partial degeneracy parameter of ($\eta \approx 2$)

The variations of the electron temperature versus ion temperature are shown in Figure (2), for different values of the magnetic field at a surface density of ρR $= 100$g$/cm^2$. It is observed that the electron temperature changes slightly for magnetic field intensity up to the order of $10^5 T$, so that the electron temperature decreases with increasing magnetic field intensity. So, by increasing the magnetic field intensity to $3.5 \times 10^5 T$ in the ion temperature range of 100 keV, the electron temperature is lower than the Fermi temperature (2.6 keV) and the plasma is in a degenerate state. On the other hand, by increasing the magnetic field intensity to $4 \times 10^5 T$, the electron temperature no longer decreases significantly, so more energy and stricter requirements must be spent on fuel ignition. Therefore, the optimal magnetic field intensity for fuel pellet ignition is considered to be about $3.5 \times 10^5 T$. Now, by obtaining the appropriate magnetic field intensity, the allowable ignition areas of the D-^{3}He fuel pellet can be obtained for the MIF state for the degenerate parameter ($\eta \approx 2$). In order to obtain the allowable ignition areas of the fuel pellet, the ignition condition equation (equation (3)) must be resolved again by applying the magnetic field intensity value.

Figure (3) shows the allowable ignition regions of D-^{3}He fuel in the MIF with a degenerate parameter ($\eta \approx 2$). It is observed that the electron temperature will decrease by 33% from the temperature range of 3.9 keV in the ICF to 2.6 keV in the MIF by applying a magnetic field intensity of $3.5 \times 10^5 T$, at an ion temperature of 100 keV and for a surface density ρR $= 100$g$/cm^2$. This way, the conditions for fuel pellet degenerate are always available. It is also observed that the surface density of the fuel pellet will reach ρR $= 500$g$/cm^2$ for the electron temperature range of 3.9 keV in the MIF. A fivefold increase in surface density will be effective in meeting the fuel pellet production and compression requirements.

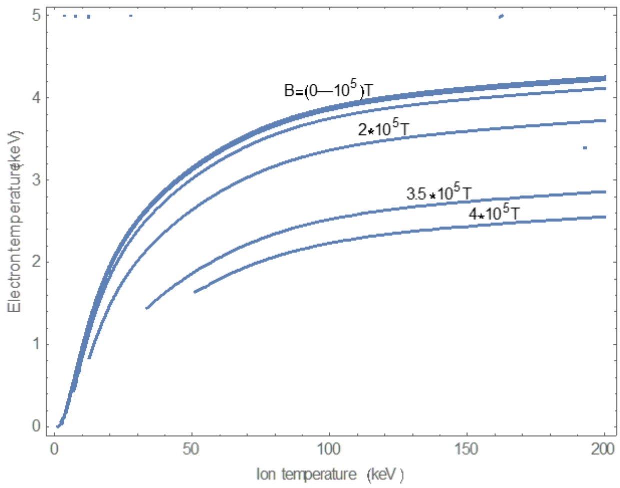

Figure 2: Electron temperature variations ion temperature at surface density ρR $=$ 100g/cm^2 of D-^{3}He fuel in MIF mode for different magnetic field strengths.

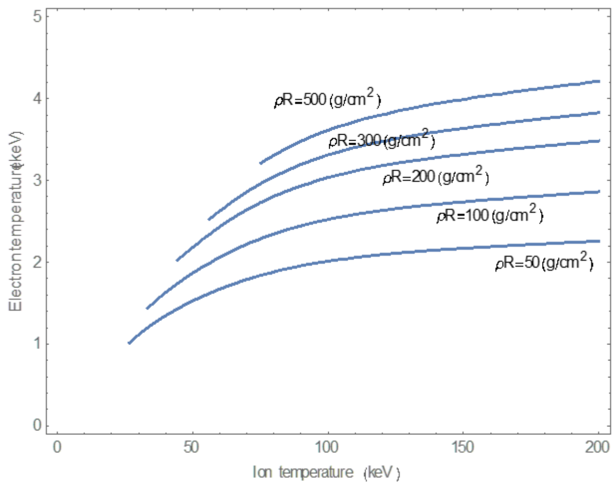

Figure 3: Change of electron temperature variations ion temperature of D-^{3}He fuel in MIF mode for partial degenerate parameter ($\eta \approx 2$)

Effects of the electron temperature anisotropy parameter on the ignition conditions and surface density of the D-^{3}He fuel pellet plasma are investigated in Figure (4). The results show (Figure (4)) that, (4a) for the ICF in the ion temperature range of 100 keV, with an increase in the temperature anisotropy parameter greater than one, ($\beta > 1$), the electron temperature is greatly reduced, so that for $\beta = 10$ the electron temperature decreases by 64% to 1.4 keV; however, for an anisotropy parameter less than 1, the plasma behavior does not change significantly. Figure (4b) For the MIF, the behavior of the partially degenerate plasma is similar to the ICF, with the difference that in the MIF, for anisotropy parameter values of $\beta = 5$, the electron temperature decreases more than in the ICF, decreasing to 1.2

keV. For $\beta = 10$, however, the electron temperature reaches 0.8 keV, even though 70% of the electron temperature has decreased because the ion temperature has exceeded 100 keV; complete fuel ignition cannot be expected in this case. Therefore, it can be concluded that in the MIF, achieving optimal fuel pellet ignition is much more likely than in the ICF. In the next part, the ignition conditions and changes in the surface density of the fuel pellet are examined for plasma in fully degenerate conditions ($\eta = 10$).

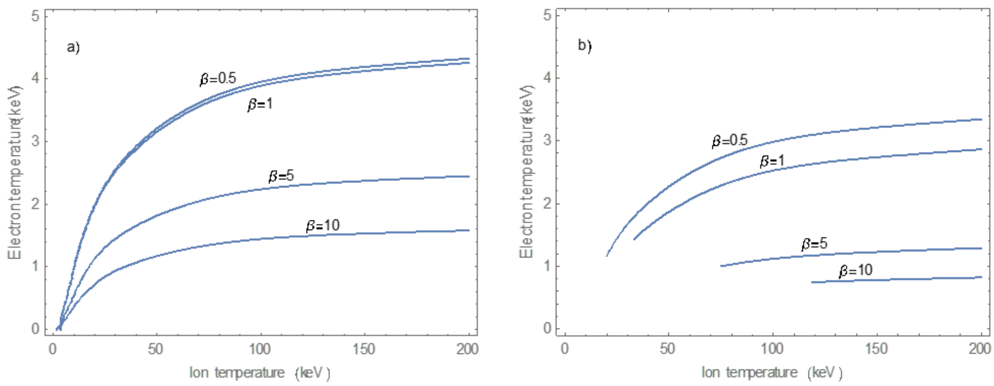

Figure 4: Electron temperature variations ion temperature for surface density ρR $=$ 100g/cm^2 D-^{3}He a) in ICF, b) in MIF in partial degeneracy mode ($\eta \approx 2$) for different temperature anisotropy parameters

As can be seen in Figure (5), the electron temperature decreases sharply with an increase in the degenerate parameter $\eta = 10$ in both ICF and MIF states, and applying a magnetic field intensity will not change the electron temperature much. In the ICF, and at an ion temperature of 100 keV, when the surface density is ρR $=$ 100g/cm^2, the electron temperature is in the range of 0.7 keV, while in the MIF state, the electron temperature is in the range of 0.65 keV with an 8% decrease. Also, the effect of temperature anisotropy parameters on the electron temperature are investigated for the ICF and MIF states with the degeneracy parameter $\eta = 10$.

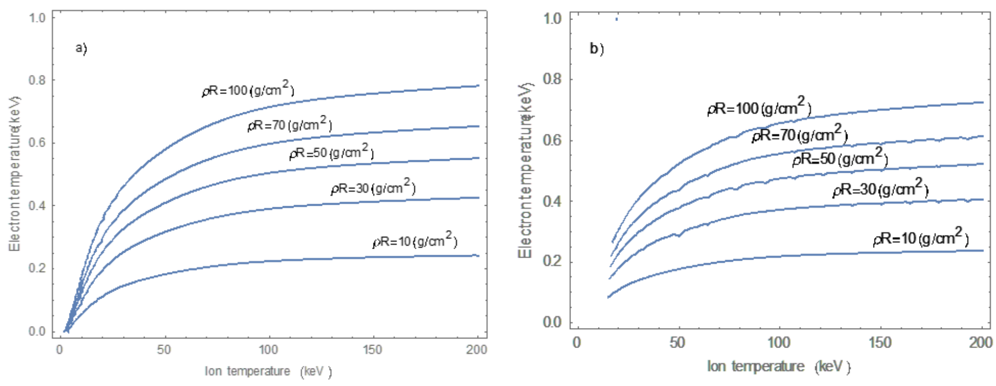

Figure 5: Electron temperature variations ion temperature of D-^{3}He fuel a) in the ICF and b) in the MIF for the degenerate parameter ($\eta \approx 10$)

According to Figure (6), it can be seen that for a degenerate parameter ($\eta = 10$), by applying a temperature anisotropy parameter (in the range of 0.5 to 1) for the D-^{3}He fuel pellet plasma, the surface density will not change much for both ICF and MIF states. However, with increasing the temperature anisotropy parameter to about $\beta = 10$, the electron temperature of the medium decreases by about 8% in the ICF state and about 16% in the MIF state. Therefore, by comparing Figures (4 and 6), it is observed that in the fully degenerate plasma condition ($\eta = 10$), the drop in electron temperature is much less than in the partially degenerate plasma condition ($\eta = 2$). In light of this, it can be said that the temperature anisotropy parameter in partially degenerate plasma conditions will have a greater effect on reducing the electron temperature than under fully degenerate plasmas.

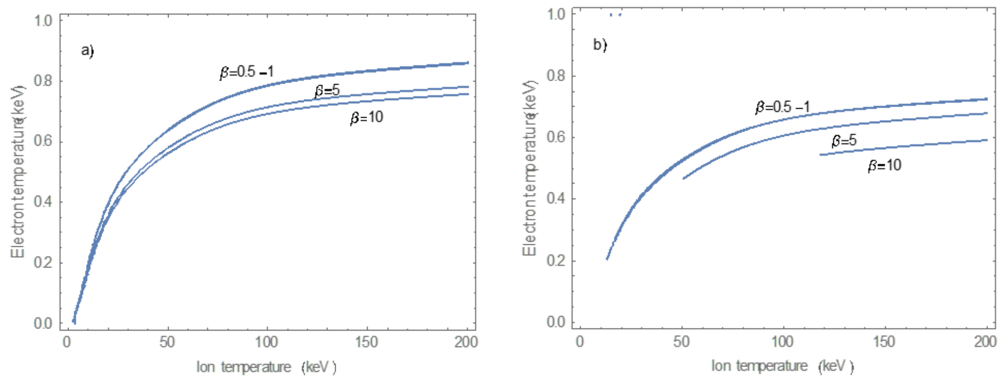

Figure 6: Electron temperature variations ion temperature of D-^{3}He fuel with surface density, ρR $= 100$g$/cm^2$ a) in the ICF, b) in the MIF for different of temperature anisotropy parameters in the degenerate state ($\eta \approx 10$)

5 Conclusion

This paper studied the effects of the degenerate parameters and temperature anisotropy on the ignition conditions of D-^{3}He fuel in ICF and MIF regimes, by calculating the generated and lost power densities. In the partially degenerate fuel pellet plasma condition ($\eta = 2$) where the plasma electron temperature is lower than the Fermi temperature, the surface density of the fuel pellet has been estimated to be ρR $= 100$g$/cm^2$ for the ICF state in the ion temperature range of 100 keV. Calculations have shown that by applying an external magnetic field $B = 3.5 \times 10^5 T$ (in the MIF state) in the partially degenerate plasma condition, the surface density of the fuel pellet increases by about 5 times compared to the ICF state. This increase in the surface density of the fuel pellet causes more alpha particle energy to be deposited into the plasma environment allowing easier access to the fuel pellet ignition conditions. Also, in the case of partial degenerate plasma, calculations show that applying temperature anisotropy to the fuel pellet reduces the electron temperature by about 70 percent in the MIF state and by about 53 percent in the ICF state. This reduction in the electron temperature of the plasma, while reducing the dissipated bremsstrahlung power, increases the ion temperature of the fuel pellet and helps achieve more suitable ignition conditions. Subsequently, the effect of these two parameters for a completely degenerate plasma has also been calculated in two states of ICF and MIF. Calculations have shown that for a completely degenerate plasma ($\eta = 10$), in a surface density condition of ρR $= 100$g$/cm^2$, the electron temperature in the MIF regime is about 8 percent lower than in the ICF regime. Furthermore, by applying a temperature anisotropy parameter of $\beta = 10$, the electron temperature decreases by about 8 percent in the ICF regime and by about 16 percent in the MIF regime. Thus, it is observed that applying a magnetic field (MIF regime), while reducing the electron temperature of the plasma environment, lowers the dissipated bremsstrahlung power and enhances the energy deposition of the fuel pellet plasma particles, thereby making the ignition conditions of the D-^{3}He fuel pellet more readily achievable.

Authors' Contributions

All authors have the same contribution.

Data Availability

No data available.

Conflicts of Interest

The authors declare that there is no conflict of interest regarding the publication of this paper.

Ethical Considerations

The authors have diligently addressed ethical concerns, such as informed consent, plagiarism, data fabrication, misconduct, falsification, double publication, redundancy, submission, and other related matters.

Funding

This research did not receive any specific grant from funding agencies in the public, commercial, or not for profit sectors.

References

[1] Nevins, W. M. 1998, J. Fusion Energy, 17, 25.

[2] McNally, J. R. 1971, Nuclear fusion, 11, 189.

[3] Wittenberg, L. J., Santarius, J. F., & Kulcinski, G. L. 1986, Fusion technology, 10, 167.

[4] Gus' kov, S. Y. 2013, Plasma Physics Reports, 39, 1.

[5] Tabak, M., Hammer, J., Glinsky, M. E., Kruer, W. L., Wilks, S. C., Woodworth, J., & Mason, R. J. 1994, Physics of Plasmas, 1, 1626.

[6] Basov, N. G., Gus' Kov, S. Y., & Feokistov, L. P. 1992, J. Soviet Laser Research, 13, 396.

[7] Atzeni, S., & Meyer-ter-Vehn, J. 2004, The Physics of Inertial Fusion: Beam Plasma Interaction, Hydrodynamics, Hot Dense Matter (No. 125). Oxford University Press.

[8] Kishony, R., & Shvarts, D. 2001, Physics of Plasmas, 8, 4925.

[9] Moses, E. I., & Wuest, C. R. 2005, Fusion Science and Technology, 47, 314.

[10] Zhang, W. Y., & He, X. T. 2008, J. Physics: Conference Series 112, 032001. IOP Publishing.

[11] Azechi, H., Mima, K., Fujimoto, Y., Fujioka, S., Homma, H., & et al. 2009, Nuclear Fusion, 49, 104024.

[12] Dunne, M. 2006, Nature physics, 2, 2.

[13] Kirkpatrick, R. C., Lindemuth, I. R., & Ward, M. S. 1995, Fusion Technology, 27, 201.

[14] Sweeney, M. A., & Farnsworth, A. V. 1981, High-gain, Nuclear Fusion, 21, 41.

[15] Pfalzner, S. 2006, An introduction to inertial confinement fusion. CRC Press.

[16] Haas, F. 2011, Quantum plasmas: An hydrodynamic approach (Vol. 65). Springer Science & Business Media.

[17] Eliezer, S., León, P. T., Martinez-Val, J. M., & Fisher, D. V. 2003, Laser and Particle Beams, 21, 599.

[18] Mahdavi, M., Bakhtiyari, M., & Najafi, A. 2023, Indian J. Physics, 97, 1277.

[19] Lindemuth, I. R. 2015, Physics of Plasmas, 22.

[20] Khodadadi Azadboni, F., Khademloo, E., & Mahdavi, M. 2023, Iranian J. Physics Research, 23, 147.

[21] Mahdavi, M., Gholami, A., & Ghodsi, O. N. 2020, Chinese J. Physics, 68, 596.

[22] Eliezer, S., Henis, Z., Nissim, N., Pinhasi, S. V., & Val, J. M. M. 2015, Laser and Particle Beams, 33, 577.

[23] Mahdavi, M., & Gholami, A. 2013, Plasma Science and Technology, 15, 323.

[24] Mahdavi, M., Bakhtiyari, M., & Najafi, A. 2023, International J. Modern Physics B, 37, 2350142.